

GABRIEL NICOLAE POPA<sup>1</sup>, IOAN ȘORA<sup>2</sup>, CORINA MARIA DINIȘ<sup>1</sup>, SORIN IOAN DEACONU<sup>1</sup>

## AN ANALYSIS ON THE VELOCITY OF DUST PARTICLES IN THE PLATE-TYPE ELECTROSTATIC PRECIPITATORS USED IN THERMOELECTRIC POWER PLANTS

Experimental data collected from different plate-type electrostatic precipitators used in a thermoelectric power plant has been analyzed. The following parameters were considered: the collection efficiency, average migration velocity of dust particles, velocity distribution of the gas in the input and output channels of precipitators. The average migration velocity of dust particles can be estimated using various mathematical models, and the gas velocity can be computed using the velocity distributions from the input channels of the precipitators. The traveling time of dust particles between the electrodes is smaller than the traveling time along the precipitator sections.

### 1. INTRODUCTION

A few different methods are used in industry to collect dust particles: gravity separation, inertial separation with cyclones, electrostatic precipitation (tube type and plate type), contacting and impaction in the case of wet scrubbers [1, 2].

For large process gas streams (more than 50 m<sup>3</sup>/s) industrial plate type electrostatic precipitators (ESPs) are used in iron, steel and glass industry. However, ESPs are mostly used in thermal power plants. ESPs can collect dust particles between 0.01 μm and 1 mm (with different efficiency) and the dust resistivity can range from 10<sup>6</sup> to 10<sup>14</sup> Ω·cm. In industry, large ESPs may have from 2 to 6 sections (usually 3 or 4), each of them having their own power supply [3].

There are different mathematical models for estimating the average migration velocity of dust particles [4, 5]: some of them do not take into account the classes of

---

<sup>1</sup>Department of Electrical Engineering and Industrial Informatics, Faculty of Engineering Hunedoara, Politehnica University of Timișoara, Revoluției str., 5, 331128, Hunedoara, Romania, corresponding author G.N. Popa, e-mail: gabriel.popa@fih.upt.ro

<sup>2</sup>Electrical Engineering Department, Faculty of Electrical and Power Engineering, "Politehnica" University of Timișoara, Bd. Vasile Pârvan, no. 2, 300223, Timișoara, Romania.

diameters of dust particles (the ones that depend on the technological parameters), and others, which take into account the diameter of dust particles by considering various classes of diameters (the ones that depend on the electric parameters) [2, 6, 7].

The dust particles trajectories can be determined, for different classes of diameters and under certain simplifying conditions (i.e. for lab or pilot ESPs), by using some complex simulation models and/or some sophisticated experimental devices (e.g. laser and high-speed video cameras) [1]. The average migration velocity in industrial plate type ESPs with multiple sections can be estimated only by using some analytical mathematical models (depending on technological parameters). The average migration velocity of dust particles gives some information about the collecting efficiency for all sections of the industrial plate ESPs. The average diameter of the dust particles collected in ESPs can be determined from the average migration velocity.

Distribution of the gas velocity in ESPs has a special importance for the ESPs' collecting efficiency. Additional experimental and numerical analyses (3D) for the distribution of gas velocity in ESPs are presented in [8, 9].

Maximum electrical charge level for dust particles can be obtained by applying maximum voltage between ESPs electrodes. In order to get optimum performance, the voltage must be automatically adjusted in accordance with charging conditions. A distributed control technique for an ESP has been presented in [10].

## 2. CLASSICAL ENERGIZATION TYPES FOR ESP SECTIONS

The main components for an ESP with three sections used in a thermoelectric power plant are presented in Fig. 1.

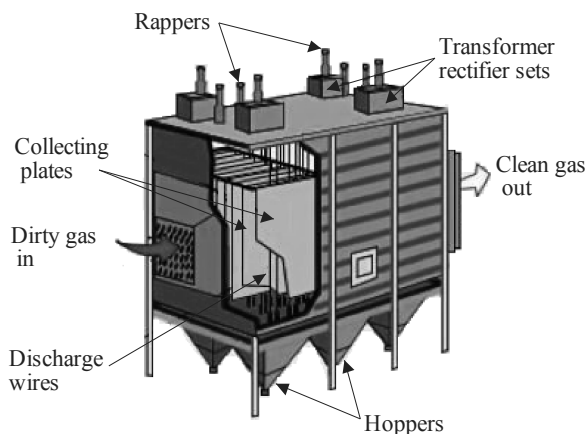


Fig. 1. Typical configuration for an industrial ESP used in a thermal power plant

Every section has its own power supply. The line voltage (two phase, 400 V AC) is controlled by a thyristor control reactor (TCR) power supply (through phase control) before it is applied to the primary side of the step-up high voltage transformer (Fig. 2). The transformer has  $n$  turns ratio to step-up the voltage to a desired level, in order to generate the corona discharge. The AC high voltage is rectified using a high voltage silicon bridge rectifier. The DC high voltage (usually up to 60 kV) is applied to each precipitator section. The discharge wires have negative polarity and the collecting plates are grounded. The firing angle of the thyristor is determined by an automatic voltage controller for every half-cycle of the low-voltage [11].

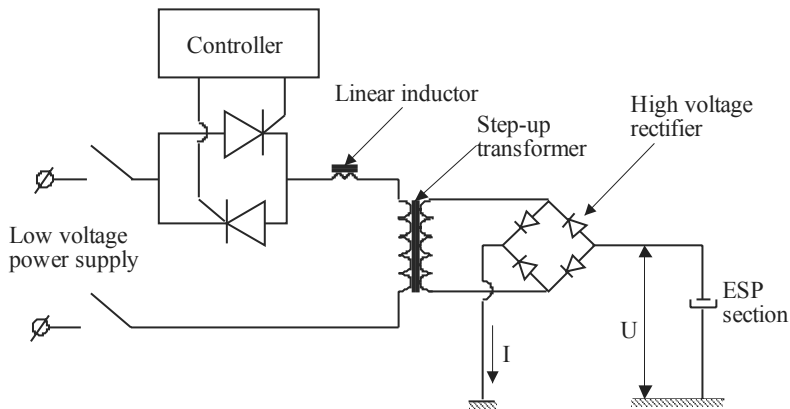


Fig. 2. Electrical power supply diagram for an ESP section

In order to control the corona discharge in each section of the ESP, the current and the voltage from low and high voltage must be measured. The current is measured with a shunt (3 A/750 mV) resistor, and the voltage with the high voltage divider (150 kV/10 V). This type of power supply has been used in the last four decades for dusts with normal resistivities between  $10^6$  and  $10^9 \Omega\text{-cm}$  [12].

### 3. COMPUTING THE COLLECTING EFFICIENCY OF INDUSTRIAL PLATE ESPs DEPENDING ON THE TECHNOLOGICAL PARAMETERS

ESPs sections are composed of many ducts containing collecting plates and discharge wires are placed inside the sections. The distance between collecting plates is  $2s$  and the distance between the collecting plates and the discharge wires is  $s$ . The dust particles flow in the  $xz$  plane, along  $y$  axis (Fig. 3). The velocity of dust particles has two components: one,  $v_p$  along  $y$  axis that it is produced by gas flow, and the other,  $w$ , (migration velocity) along  $x$  axis, that is produced by electric forces existing between the electrodes.

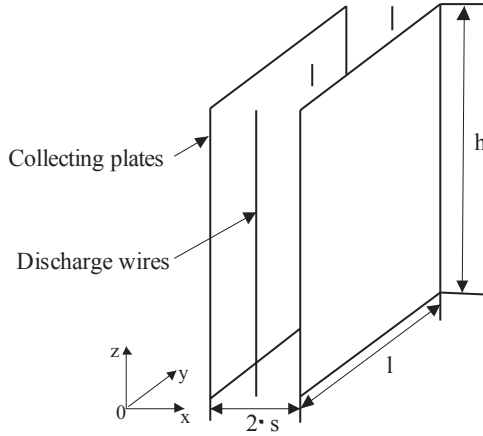


Fig. 3. A single duct from an ESP section

It is assumed that  $m_p$  is the weight of a dust particle,  $v_p$  is its moving velocity inside the section,  $t$  is the time,  $q_p$  is electrical charge of a dust particle,  $E_p$  is the electrical field strength,  $d$  is the diameter of a dust particle, and  $\mu$  is the dynamic viscosity.

The movement of particles [1] can be determined by solving the equation:

$$m_p \frac{dv_p}{dt} = q_p E_p - 3\pi d \mu v_p \quad (1)$$

Its solution is:

$$v_p(t) = \frac{q_p E_p}{3\pi d \mu} \left(1 - e^{-3\pi d \mu t / m_p}\right) \quad (2)$$

In the steady-state regime, the particles reach the following velocity:

$$v_p = \frac{q_p E_p}{3\pi d \mu} \quad (3)$$

Assuming that  $q_i$  is the inlet dust concentration and  $q_o$  is the outlet dust concentration for electrostatic precipitators, the plate-type electrostatic precipitator collecting efficiency  $\eta$  is defined as:

$$\eta_l = 1 - \frac{q_o}{q_i} \quad (4)$$

Let us consider a plate-type electrostatic precipitator with  $n$  sections. Practically, the maximum number of sections is 10. At the outlet of  $(n - 1)$ th section, the dust concentration is  $q_{n-1}$  (Fig. 4). The collecting efficiency  $\eta_l$  of the section 1 is:

$$\eta_1 = 1 - \frac{q_1}{q_i} \quad (5)$$

The collecting efficiency  $\eta_2$  of the section 2 is:

$$\eta_2 = 1 - \frac{q_2}{q_1} \quad (6)$$

The collecting efficiency  $\eta_n$  of the section n is:

$$\eta_n = 1 - \frac{q_f}{q_{n-1}} \quad (7)$$

From Eqs. (5)–(8), the total collecting efficiency is:

$$\eta = 1 - (1 - \eta_1)(1 - \eta_2) \dots (1 - \eta_n) \quad (8)$$

The total collecting efficiency depends on the collecting efficiency of every section.

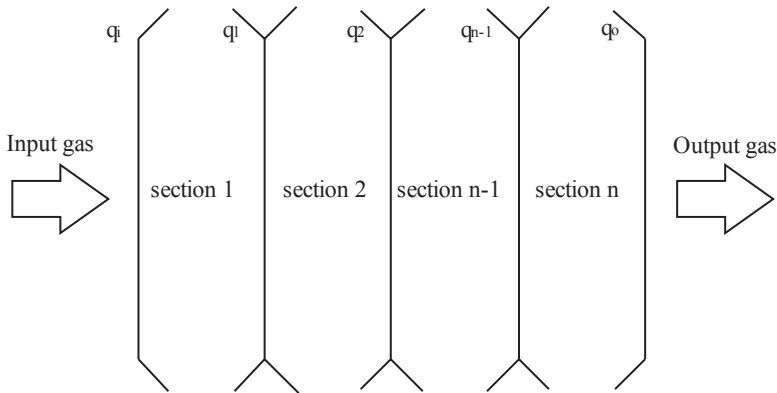


Fig. 4. Collection of particles in an ESP with  $n$  sections

If  $\alpha$  is the specific collecting surface,  $S$  is the total ESP's collecting surface and  $Q$  is gas flow:

$$\alpha = \frac{S}{Q} \quad (9)$$

The collecting efficiency  $\eta$  depends on the average migration velocity of the dust particles  $w$  and specific collecting surface  $\alpha$ :

$$\eta = 1 - e^{-wS_c/Q} = 1 - e^{-w\alpha} \quad (10)$$

Equation (10) was first derived by Deutsch [13] and it provides the efficiency value for a very simplified ESP model [1, 2].

If  $n_s$  is the number of sections,  $l_i$  is the length of the section,  $h_i$  is the height of the section,  $n_{di}$  is the number of ducts in the sections, the total ESP's collecting surface is:

$$S = \sum_{i=1}^{n_s} S_i = \sum_{i=1}^{n_s} l_i h_i (2(n_{di} - 1) + 2) \quad (11)$$

An improvement for this model was first proposed by Matts and Öhnfeld [14]:

$$\eta = 1 - e^{-(w\alpha)^{1/\chi}} \quad (12)$$

(where typically  $\chi = 0.1-0.8$ ). This equation can only be used when the electrical conditions in ESPs are maximized.

Another improvement was made in [1], where in most cases  $\lambda \leq 0.22$ :

$$\eta = 1 - \frac{1}{(1 + \lambda w\alpha)^{1/\lambda}} \quad (13)$$

#### 4. SIMULATED RESULTS OF AVERAGE MIGRATION VELOCITY

An approximate estimation of the average migration velocity can be calculated if the inlet  $q_i$  and outlet  $q_o$  dust concentrations, and the total collecting surface of the collecting plates  $S$  and the gas flow  $Q$  are known. From Eq. (10) it results:

$$w = -\frac{1}{\alpha} \ln(1 - \eta) \quad (14)$$

and the average migration velocity of dust particles in the ESP can be computed from this equation. Using other models, from Eq. (12) the migration velocity can be calculated as:

$$w = -\frac{1}{\alpha} (\ln(1 - \eta))^{1/\chi} \quad (15)$$

From the latter model, Eq. (13), the migration velocity can be calculated as:

$$w = \frac{1}{\lambda\alpha} \left[ \left( \frac{1}{1-\eta} \right)^\lambda - 1 \right] \quad (16)$$

For example, the average migration velocity of dust particles using real data from a thermal power station (S.C. Electrocentrale Deva S.A., Romania) where hundreds of thousands of m<sup>3</sup>/h of gas are treated (i.e. 650 000 m<sup>3</sup>/h) has been calculated. The power plant has six power sections (210 MW) each connected to a boiler and it has twelve ESPs (with three and four sections). The main geometrical data of precipitators used at the thermal power station are given in Table 1 [11].

Table 1

The total collecting surfaces of some ESPs

Parameter	ESP 1 (A or B)	ESP 4 (A or B)	ESP 5 (A or B)	ESP 6 (A or B)
Number of ducts	46	54	55	56
Height h, m	12			
Section length l, m	4.32			
Surface area of section $S_{\text{section}}$ , m <sup>2</sup>	4769.28	5598.72	5702.4	5806.08
Number of sections $n_c$	4	3		
Total surface of ESP $S_{\text{tot}}$ , m <sup>2</sup>	19 077.12	16 796.16	17 107.2	17 418.24

During this time, ESPs with 2, 3, and 4 sections (operating at different times) were used in various control conditions and power supply types (Table 2) [15–24].

Table 2

Calculated collecting efficiencies ( $\eta$ ), gas flows ( $Q$ ), average gas velocities ( $v$ ), and the specific collecting surfaces ( $\alpha$ ) for a plate ESP

ESP No. case	$q_i$ [g/m <sup>3</sup> ]	$q_o$ [g/m <sup>3</sup> ]	$\eta$ Eq. (10)	$Q$ [m <sup>3</sup> /s]	$v$ [m/s]	$\alpha$ [m <sup>2</sup> /(m <sup>3</sup> /s)]
1A a	24.27	0.059	0.9976	123.62	0.64	154.32
1B b	22.235	0.06	0.9973	114.65	0.593	166.39
1A c	24.61	0.056	0.9977	114.4	0.592	166.76
1B d	20.84	0.053	0.9975	107.65	0.557	177.21
1A e	26.915	0.083	0.9969	119.01	0.616	160.30
1B f	28.795	0.085	0.997	115.2	0.596	165.60
1A g	26.915	0.08	0.997	119.01	0.616	160.30
1B h	28.795	0.092	0.9968	115.2	0.596	165.760
4A a	25.528	0.138	0.9946	137.71	0.708	121.97
4A b	15.498	0.562	0.9637	137.71	0.708	121.97

Table 2

Calculated collecting efficiencies ( $\eta$ ), gas flows ( $Q$ ), average gas velocities ( $v$ ), and the specific collecting surfaces ( $\alpha$ ) for a plate ESP

4A c	24.127	0.154	0.9936	137.71	0.708	121.97
4B d	24.908	0.147	0.9941	130.23	0.67	128.97
4A e	43.905	0.123	0.9972	111.02	0.571	151.29
4A f	43.905	0.146	0.9967	111.02	0.571	151.29
5A a	20.061	0.198	0.9901	111.62	0.563	153.26
5B b	20.746	0.187	0.991	140.3	0.708	121.93
5B c	32.777	0.7775	0.9763	168.72	0.852	101.39
5B d	38.184	0.6974	0.9817	123.01	0.621	139.07
6A a	26.464	0.113	0.9957	125.2	0.621	139.12
6B b	20.953	0.167	0.992	128.37	0.636	135.69

The average migration velocities (using Eqs. (10), (12) and (13), calculated based on the data from industry) are given in Tables 3 and 4. The collecting efficiencies for all the case studies are above 0.97 (in the most cases above 0.99). The dust particles with the diameter over 10  $\mu\text{m}$  are collected better than smaller ones.

Table 3

Computed average migration velocities  $w$  [cm/s]  
assuming  $\chi = 0.2-0.8$

ESP No. case	Eq. (13)	Eq. (14)			
		$\chi = 0.2$	$\chi = 0.4$	$\chi = 0.6$	$\chi = 0.8$
1A a	3.909	0.928	1.330	1.905	2.729
1B b	3.555	0.858	1.224	1.746	2.491
1A c	3.643	0.860	1.234	1.770	2.539
1B d	3.381	0.807	1.155	1.652	2.363
1A e	3.603	0.886	1.258	1.787	2.537
1B f	3.508	0.859	1.221	1.735	2.467
1A g	3.624	0.887	1.261	1.793	2.549
1B h	3.469	0.857	1.215	1.724	2.445
4A a	4.281	1.141	1.588	2.210	3.076
4A b	2.719	1.042	1.324	1.683	2.139
4A c	4.142	1.134	1.567	2.167	2.996
4B d	3.980	1.075	1.492	2.069	2.869
4A e	3.885	0.942	1.342	1.913	2.726
4A f	3.777	0.937	1.327	1.881	2.665
5A a	3.011	0.886	1.203	1.633	2.218
5B b	3.863	1.118	1.524	2.078	2.834
5B c	3.691	1.284	1.672	2.177	2.835
5B d	2.877	0.949	1.252	1.652	2.180
6A a	3.917	1.009	1.416	1.988	2.790
6B b	3.558	1.010	1.383	1.896	2.597

Table 4

Computed average migration velocity  $w$  [cm/s] for dust particles from Eq. (17) for various  $\lambda$

ESP No. case	$\lambda = 0.22$	$\lambda = 0.1$	$\lambda = 0.01$	$\lambda = 0.001$	$\lambda = 0.0001$
1A a	8.159	5.366	4.029	3.921	3.910
1B b	7.304	4.848	3.662	3.565	3.556
1A c	7.647	5.012	3.756	3.654	3.644
1B d	7.019	4.630	3.484	3.391	3.382
1A e	7.270	4.877	3.710	3.614	3.605
1B f	7.108	4.756	3.612	3.518	3.509
1A g	7.343	4.914	3.731	3.635	3.625
1B h	6.969	4.687	3.571	3.479	3.470
4A a	8.028	5.621	4.395	4.292	4.282
4A b	4.003	3.224	2.764	2.723	2.719
4A c	7.597	5.389	4.248	4.152	4.143
4B d	7.377	5.201	4.084	3.990	3.981
4A e	7.945	5.288	4.002	3.897	3.886
4A f	7.556	5.094	3.887	3.788	3.778
5A a	5.221	3.827	3.082	3.018	3.012
5B b	6.780	4.935	3.956	3.872	3.864
5B c	5.729	4.476	3.761	3.698	3.692
5B d	4.613	3.537	2.935	2.883	2.877
6A a	7.567	5.207	4.025	3.927	3.918
6B b	6.341	4.574	3.646	3.567	3.559

Each line of Tables 2–4 presents a distinct practical operation case. The ESPs number and the operation case a, b, c, etc. appear in the header of each line in the first column.

Equations (15) and (16) were used to simulate different values for the coefficients  $\chi$  and  $\lambda$ . In Tables 2–4 20 operation cases are given compared (each case has no connection with the other cases) for eight industrial ESPs (generic No. 1A, 1B, 4A, 4B, 5A, 5B, 6A, and 6B). Each section of the ESPs is supplied from a classic power source (thyristor control reactor, Fig. 2). In all the cases and for all the sections, the automatic regulators of the supply power sources have ensured maximum adjusted currents in the corresponding sections.

Collecting efficiencies are usually over 99% (Table 2), with higher values for four-section ESPs (1A and 1B). The percentage of small dust (up to 100%) that remains uncollected is determined from particles with very small diameters (below 2.5  $\mu\text{m}$ ) [2]. It can be noted that in all the cases where the flows have high values, the gas velocities inside the precipitator are usually below 0.85 m/s.

The average migration velocities are in the order of a few cm/s (2.7–4.3 cm/s). The calculations were not performed for all the groups and all the classes of diameters

of the dust particles because the mathematical models from Eqs. (14)–(16) are irrelevant. The smaller the particle diameters, the smaller the migration velocity was.

As can be seen from Eq. (15), the parameter  $\chi$  strongly influences the calculated value of the average migration velocity. For  $\chi = 0.2$ , the migration velocities are below 1.2–1.3 cm/s, but if  $\chi = 0.8$  they increase to 2.2–3 cm/s and tend towards the values calculated from Eq. (15).

The coefficient  $\lambda$  in the mathematical model (Eq. (16)) is usually below 0.22. Three groups of migration velocities for five  $\lambda$  coefficients were determined. In all cases, the migration velocities are in the order of a few cm/s. For  $\lambda = 0.22$ , the velocities exceed 4 cm/s and are up to 8.2 cm/s. Once  $\lambda$  decreases, the migration velocities become smaller. It can be noticed that for  $\lambda = 0.0001$ , the migration velocities are comparable (almost identical) with the ones calculated from Eq. (14). Thus, it can be concluded that for the mathematical models based on Eq. (14) and on Eq. (16), the results are similar (depending on  $\lambda$ ). Usually, the distance between electrodes (the discharge wires and the collecting plates) for an industrial precipitator is 15–17.5 cm. If the average migration velocity is 3 cm/s (minimum value) then, that distance between electrodes can be traveled by charged dust particles in time intervals ranging from 5 s to 6 s.

## 5. TECHNOLOGICAL MEASUREMENTS UPON SOME PARAMETERS

The characteristics of bituminous coal used in the thermo electric power plant (S.C. Electrocentrale Deva S.A., Romania) is presented in Table 5 [11].

Table 5

Characteristics of the used fuel (bituminous coal)

Parameter	Rated values	Limit values
Net calorific power, kcal/kg	2750	2450
Ash resulted after burning, %	50.3	54.5
Humidity, %	10	10
Sulphur content, %	1.8	1

This thermal power station has ESPs with three or four sections that treat large gas flows. Because of this, every ESP has two inlet channels connected to the boiler and one single outlet channel (Fig. 5).

In order to establish the collection efficiency, the measurements of the velocity distribution and the dust concentration of the waste gas were done simultaneously at the inlet and the outlet of the ESP ( $xz$  plane, Fig. 5). The measuring sockets were placed in the available places, distributed as follows:

- in the inlet channels: 4 sockets on each branch noted 1, 2, 3, 4;
- in the outlet channel: 12 sockets noted 1, 2, ..., 12.

Each tube contained 11 measuring points marked from top to bottom as S1, S2, ..., S11.

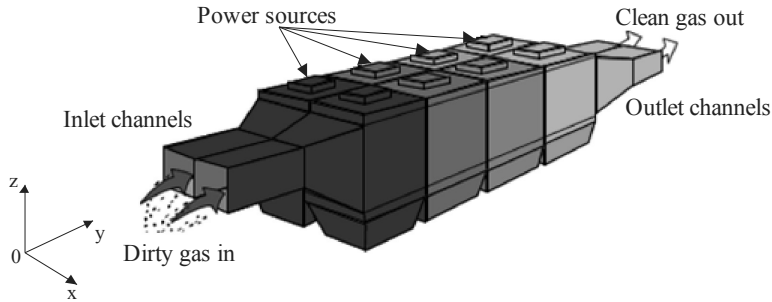


Fig. 5. Inlet channels (for dirty gas in) and outlet channels (for gas out) of large ESPs from thermoelectric power plants

The gas velocities at various points were determined by using a Pitot–Prandtl tube and differential micro-manometer in the measurement sockets placed in the inlet and outlet branches. In such experiment a Pitot–Prandtl tube is used to measure the total pressure  $p_0$  and the static pressure  $p_s$ , which are determined by the velocity of the gas flowing through the channels. By means of a differential micro-manometer the difference of pressures,  $p_0 - p_s$  is measured, being proportional with the gas velocity [18, 19]. The measurements were performed in the regime of maximum technological load of the boiler. The inlet and outlet channels have a smaller surface than the surface of the ESPs sections. Thus, the velocity inside the precipitator is smaller (below 1 m/s).

At the inlet channels, for the two ESPs (4A and 4B), in Figs.6 and 8, the velocities of the inlet branches (7–15 m/s) are higher than at the outlet branch (5–11 m/s). This is due to the larger cross-section at the ESP's outlet.

At the inlet branches in Figs. 6 and 8, the gas velocities are higher in the central area and towards the upper parts of the channels. The distribution of the gas velocity at the inlet of the ESP is non-uniform, even if leveling devices were used at the inlet [2].

Gas distribution at the input sections of the ESP is almost the same as the distribution at the input channels. Gas velocities at various points of the cross section have lower values (<1 m/s) due to the fact that the transversal cross section area is much larger than the area of the input channels. Less important, from the operation's viewpoint, is the gas velocities distribution at the outlet of the ESP (Figs. 7 and 9). In general, the highest velocities (10–14 m/s) can be observed in the central and upper area. It has been found that the velocities at the inlet of ESP 4A are smaller than the velocities at the inlet of ESP 4B, due to the fact that the measurements were not performed at the same time.

The length of an industrial precipitator ranges from 13 m to 18 m, depending on the length of the section and the number of sections. This distance can be covered by dust particles in 15 to 21 s, a longer period than the time needed to charge and collect the dust particles. Theoretically, there is enough time for the dust particles to travel between the electrodes, but another phenomenon appears: the turbulence of the gas.

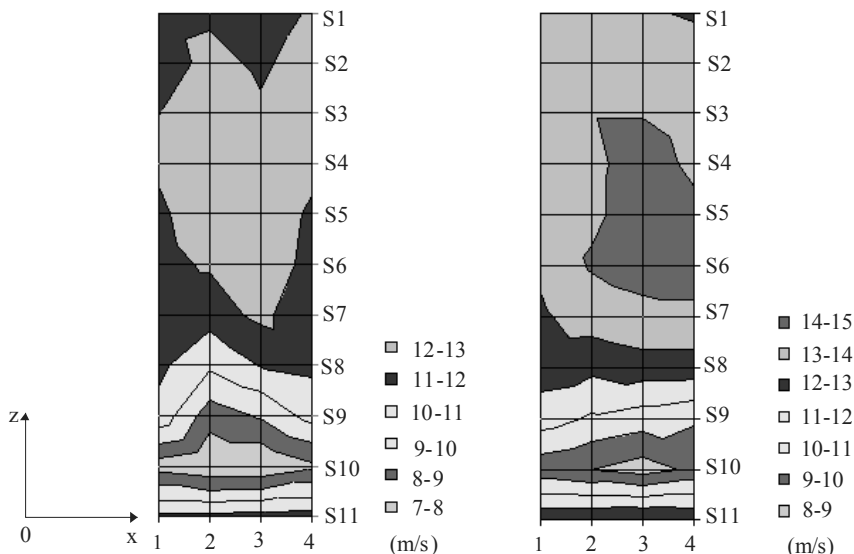


Fig. 6. Velocity distribution in the input section of ESP 4A

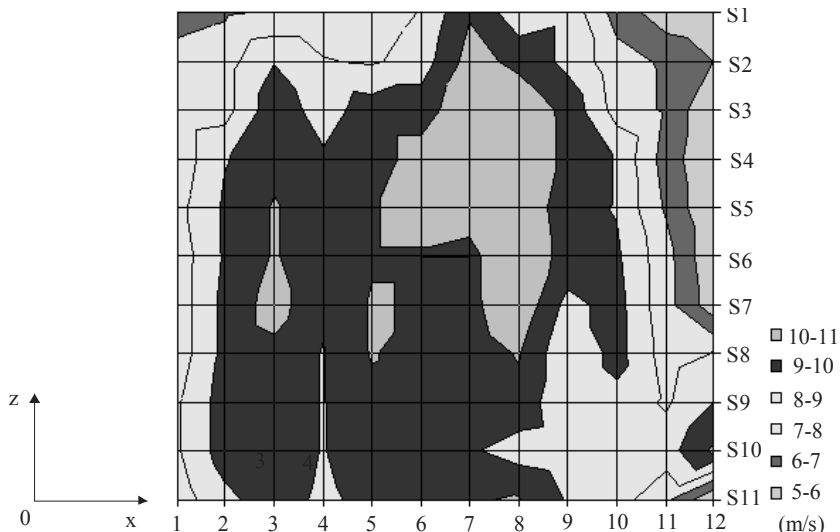


Fig. 7. Velocity distribution in the output section of ESP 4A

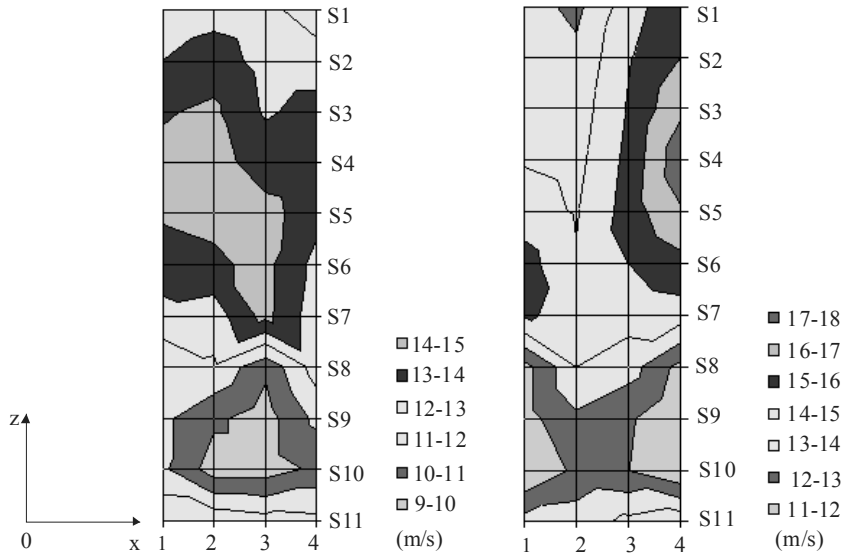


Fig. 8. Velocity distribution in the input section of ESP 4B

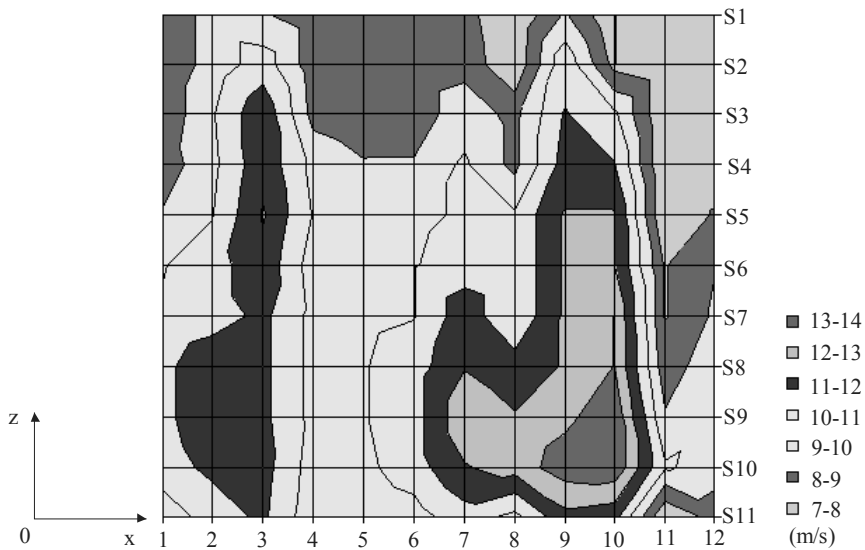


Fig. 9. Velocity distribution in the output section of ESP 4B

The gas turbulence can be expressed mathematically only from a statistical aspect. Inappropriate design of the inlet connectors, improper construction of the gas leveling grid, wrong placement of the installations within the technological process, too small sections of the channels with wrong shapes, dust depositions that could clog future

passes will cause a non-uniform gas velocity distribution, which in turn leads to a poor dust collection [12].

Steam flow production depends on the boiler load and the quantity of burnt coal. A larger quantity of coal in the boiler will cause an increase in the flow of the steam produced (used for the turbine) and also an increase in waste gases and dust. In Figures 10 and 11, the dependences of dust emission at the exit of the ESP with three plates (ESP 3A and 3B) on the flow rate of the steam are shown. In the figures, the lines indicating the evolutionary regression were also plotted. Dust emissions in Fig. 11 are smaller because a smaller quantity of coal is burnt.

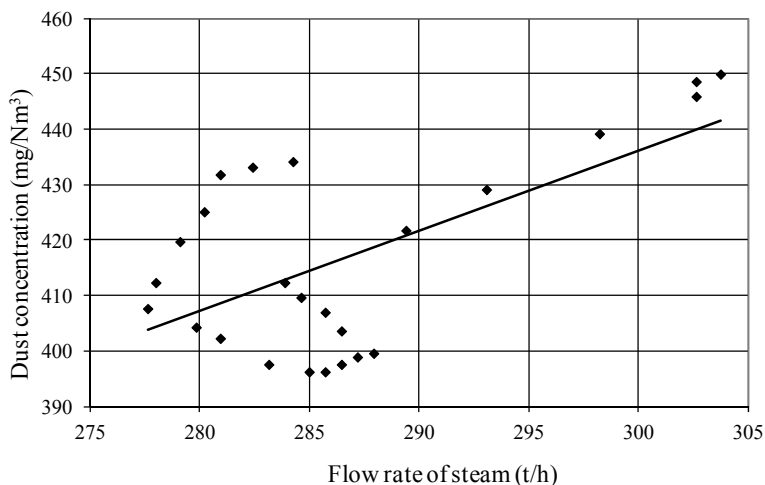


Fig. 10. Dependence of the dust concentration on the steam flow rate for ESP 3A

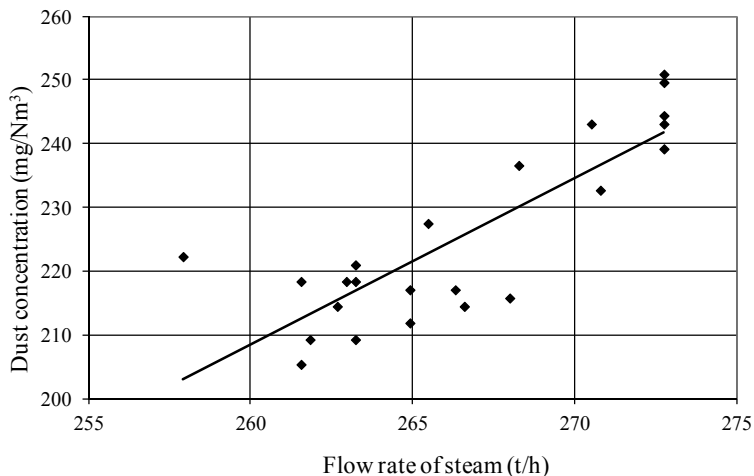


Fig. 11. Dependence of the dust concentration on the steam flow rate for ESP 3B

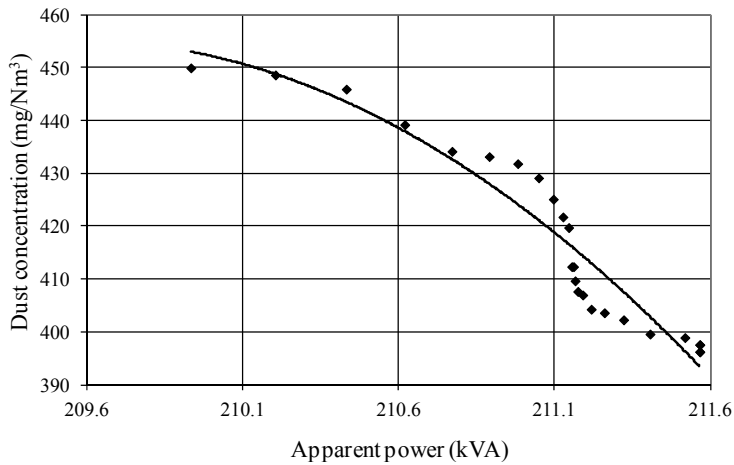


Fig. 12. Dependence of the dust emission on the apparent power for ESP 3A

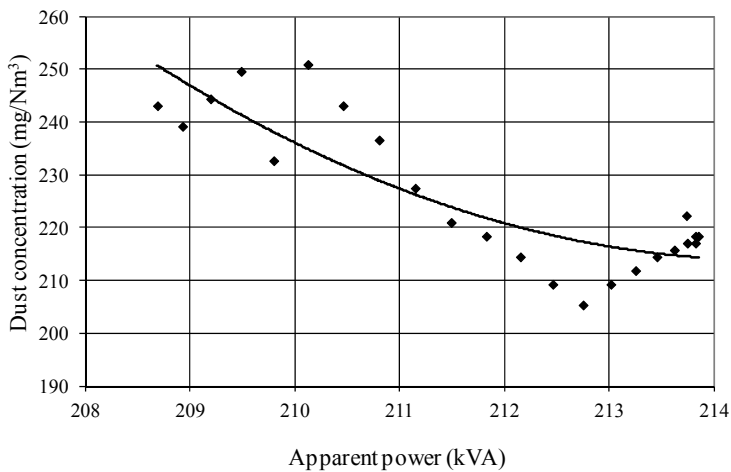


Fig. 13. Dependence of the dust emission on the apparent power for ESP 3B

Figures 12 and 13 present the dependences of the emissions of dust on the average apparent power. For both ESP 3A and 3B, the reduction of the dust emissions results in a small increase of the apparent power [25].

## 6. DISCUSSION

With a relatively simple construction, easy operation and possibility of complete automation of the dedusting process, these ESPs are used in removing solid particles

from industrial flue gases, including ash from waste gases produced by the steam boilers in thermo-electric power plants that burn coal.

From an operational viewpoint, the ESP represents a unitary whole, with independent electrical and mechanical parts. Any malfunction of an individual part reduces the collection efficiency, which depends on the following factors:

- keeping the parallelism and the distances between the discharge wires and collecting plates,
- shaking the sections over time, with higher frequency for the inlet sections of the ESP and smaller frequency for the outlet sections,
- shaking periodically the discharge wires,
- continuous removal of the collected dust.

The ESPs operation can be brought into an optimal regime in situations where all the power consumers (rappers, heaters of discharge wires, insulators, high voltage equipment) are very well controlled. This is achieved by using PLCs to control and monitor the operation of ESPs.

A relatively high level of automation of the electrostatic cleaning process of the waste gas can be achieved for the auxiliary control and command equipments of ESPs. During the operation of any boiler assembly, the volume and composition of the waste gases can vary, which can be caused by:

- burning of diverse types of coals, with different ash content,
- incidents or some anomalies in the operation of the coal mills,
- modification of the boilers' operation.

The gas velocity must be lower than the velocity of the charged dust particles to be collected. Usually, in large ESPs the gas velocity is below 1 m/s. The average migration velocity is a factor that depends on the electrical conditions (type of power supply, the amplitude and shape of the voltage, current control inside sections) of the precipitator sections. In practice, it is difficult to measure the migration velocity; the only viable method is to estimate it using mathematical models. For large precipitators, the average migration velocity is typically below 6 cm/s.

Due to the complex phenomena in ESPs, all the parameters that affect the production of the contaminated gas should be taken into account. An important aspect refers to the avoidance of the re-entrainment phenomenon, while shaking the sections, and minimizing the back corona effect.

## 7. CONCLUSIONS

The average migration velocity of dust particles (the same for all classes of particles) in ESPs was computed using three models with different collecting efficiency.

From the simulated cases it can be noted that the migration velocity is of the order of a few cm/s (3–6 cm/s). The average diameter of dust particles can be determined for

a certain type of ashes (in this case the dust particle average diameter is in the  $\mu\text{m}$  range) by knowing the average migration velocity and the dependence between the migration velocity and the average diameter of dust particles. The migration velocity  $w$  is considered a general parameter of the electrical performance and automation, and represents the bridge between the electrical power supply and the ESPs' collecting efficiency. The migration velocity cannot be determined experimentally, it can only be estimated from the existent mathematical models. Simulations were performed in order to obtain the data for the industrial plate ESPs from a thermal power station. For a more detailed analysis, electrical power supply mode should also be taken into account. Due to the combustion of the gas boiler, the gas has a non-uniform velocity distribution at the input of the ESP. The gas displacement at the transversal cross section of the ESP is non-uniform. The time required for the charged dust particles to travel between the electrodes is smaller than the time required to travel along the precipitator's length.

#### ACKNOWLEDGEMENT

This paper was supported by the project *Development and support of multidisciplinary postdoctoral programmes in major technical areas of national strategy of Research – Development – Innovation 4D-POSTDOC*, contract No. POSDRU/89/1.5/S/52603, co-funded by the European Social Fund through Sectorial Operational Programme Human Resources Development 2007–2013.

#### REFERENCES

- [1] PARKER K.R., *Applied Electrostatic Precipitators*, Chapman and Hall, London, UK, 1997.
- [2] PARKER K.R., PLAKS N., *Electrostatic Precipitator (ESP) Training Manual*, United States Environmental Protection Agency, EPA-600/R-04-072, U.S.A., 2004.
- [3] POPA G.N., VAIDA V., ABRUDEAN C., DEACONU S.I., POPA I., *A Case Study of ESP Electrical Characteristics from a Thermal Power Station*, IEEE 44th IAS Annual Meeting, Houston, Texas, U.S.A., October 4–8, 2009, 1–6.
- [4] LAMI E., MATTACHINI F., SALA R., VIGL H., *A Mathematical Model of Electrostatic Section in Wires-Plate Electrostatic Precipitators*, J. Electrostat., 1997, 39, 1–21.
- [5] LOWLESS P.A., *ESPVI 4.0. Electrostatic Precipitator V-I Performance Model-User's Manual*, Center for Aerosol Technology, Research Triangle Institute, Durham, NC, U.S.A., 1996.
- [6] BRANC M., HORÁK J., OCHODEK T., *Fine Particle Emissions from Combustion of Wood and Lignite in Small Furnaces*, Environ. Prot. Eng., 37 (2), 2011, 123–132.
- [7] BOGACKI M., OLENIACZ R., MAZUR M., KAMIŃSKI S., *Real-Time Measurement of the Size of Air Particulates*, Environ. Prot. Eng., 32 (3), 2006, 69–73.
- [8] PIEKARSKA K., ZACIERA M., CZARNY A., ZACZYŃSKA E., *Application of Short-Term Tests in Assessment of Atmospheric Air Pollution*, Environ. Prot. Eng., 37 (2), 2011, 85–98.
- [9] LÉGER L., MOREAU E., TOUCHARD G., *Effect of a DC Corona Electrical Discharge on the Airflow Along a Flat Plate*, IEEE T. Ind. Appl., 2002, 38 (6), 1478–1485.
- [10] DURGA PRASAD N.V.P.R., LAKSHMINARAYANA T., NAROSIMHAM J.R.K., VERMAN T.M., KRISHNAM RAJU C.S.R., *Automatic Control and Management of Electrostatic Precipitator*, IEEE T. Ind. Appl., 1999, 35 (3), 561–567.

- [11] POPA G.N., VAIDA V., DEACONU S.I., SORA I., *An Analysis of the Optimal Fields Number of the Plate-Type Electrostatic Precipitators Used in Thermoelectric Power Plant*, Optimization of Electrical and Electronic Equipment, IEEE OPTIM 2010, Moeciu-Bran, Braşov, Romania, May 20–22, 2012, 232–239.
- [12] POPA G.N., *Performances Improving Contributions for Some ESPs with Bi-Phasic Systems Gases –Solid Particles*, Ph.D. dissertation, Electrotechnical Faculty, Politehnica University, Timişoara, Romania, 2004 (in Romanian).
- [13] DEUTSCHW., *Bewegung und Ledung der Elektrizitatstrager in Zylinder Kondensator*, Ann. Physik, 68, Leipzig, Germany, 1922, 335–344 (in German).
- [14] MATTS S., ÖHNFELDT O.P., *Efficient Gas Cleaning with the SF Electrostatic Precipitator*, Flakten Rev., 6, 1963, 93–110.
- [15] MACARIE R., *Measuring for Establish the Collection Efficiency at Electrical Un-dusting Installation, Energetic Group, No. 1 from Thermoelectric Power Plant Mintia-Deva*, Research project 2181-CPPM, S.C. ICPET S.A., Bucharest, Romania, 1996 (in Romanian).
- [16] GLODEAN N., *Operation Behaviour of ESP from Thermoelectric Power Plant Mintia-Deva*, research project 3271/86, ICEMENERG, Bucharest, Romania, 1986 (in Romanian).
- [17] MOŢIU C., *Tests to Establish the Un-dusting Parameters of ESPs with Two Sections from Thermoelectric Power Plant Mintia-Deva*, Research project ICSIT 2005-CE, ICEMENERG, Bucharest, Romania, 1993 (in Romanian).
- [18] HERLEA M., *Operations Optimization of ESPs from Group No.4, with Three Sections*, Research project 7815-2, S.C. ICPET S.A., Bucharest, Romania, 1998 (in Romanian).
- [19] MACARIE R., *Electrical Un-dusting Installation for Group No. 4, from Thermoelectric Power Plant Mintia-Deva*, Research project 2131-CPPM, S.C. ICPET S.A., Bucharest, Romania, 1995 (in Romanian).
- [20] MACARIE R., *Measuring for Establish the Collection Efficiency at Electrical Un-dusting Installation, Energetic Group, No.5 from Thermoelectric Power Plant Mintia-Deva*, Research project 2161-CPPM, S.C. ICPET S.A., Bucharest, Romania, 1996 (in Romanian).
- [21] MACARIE R., *Electrical Un-dusting Installation for Group No. 6, from Thermoelectric Power Plant Mintia-Deva*, Research project 2130-CPPM, S.C. ICPET S.A., Bucharest, Romania, 1995 (in Romanian).
- [22] HERLEA M., *Operations Optimization of ESPs from Group No. 1, with Four Sections*, Research project 7815-1, S.C. ICPET S.A., Bucharest, Romania, 1998 (in Romanian).
- [23] MACARIE R., *Measuring for Establish the Collection Efficiency at Electrical Un-dusting Installation, Energetic Group No. 1, IDE 1300000 m<sup>3</sup>/h, from Thermoelectric Power Plant Mintia-Deva*, Research project 2161-CPPM, S.C. ICPET S.A., Bucharest, Romania, 1996 (in Romanian).
- [24] MACARIE R., *Tests to Establish the Un-dusting Parameters IDE 1300000 m<sup>3</sup>/h, Energetic Group No. 1 from Thermoelectric Power Plant Mintia-Deva*, Research project 2162-CPPM-3, S.C. ICPET S.A., Bucharest, Romania, 1996 (in Romanian).
- [25] POPA G.N., DEACONU S.I., POPA I., DINIŞ C.M., *Experimental Analysis for Plate-Type Electrostatic Precipitators with Three Sections, Optimization of Electrical and Electronic Equipment*, IEEE OPTIM 2012, Cheile Grădiştei, Braşov, Romania, May 24–26, 2012, 1274–1279.